UNIVERSITY OF LEEDS

Article:
Soltani, S, Kasaeian, A, Sarrafha, H et al. (1 more author) (2017) An experimental investigation of a hybrid photovoltaic/thermoelectric system with nanofluid application. Solar Energy, 155. pp. 1033-1043. ISSN 0038-092X

https://doi.org/10.1016/j.solener.2017.06.069

An Experimental Investigation of a Hybrid Photovoltaic/Thermoelectric System with Nanofluid Application

Shohreh Soltani[1], Alibakhsh Kasaeian[2]*, Hamid Sarrafha[3] Dongsheng Wen[4,5]

[1,2,3]Department of Renewable Energies, Faculty of New Science & Technologies, University of Tehran, Tehran, Iran.

4. School of Aeronautic Science and Engineering, Beihang Unviersity, Beijing

5. School of Chemical and Process Engineering, University of Leeds.

Corresponding Authors: akasa@ut.ac.ir, d.wen@buaa.edu.cn Tel: +98 9121947510, Fax: +98 21 88497324

Abstract

Improving photovoltaic efficiency is fundamental to the large scale utilization of solar energy and reduction of carbon emission. In this field, reducing the temperature of the Photovoltaic (PV) panel will increase its efficiency and power production. Utilizing hybrid photovoltaic/thermoelectric (PV/TE) systems is a useful way to simultaneously release the excess heat of the PV panel and using this heat to produce power. The cooling method used for the thermoelectric module (TEM) plays an important role in the system efficiency as well as the produced power. A new nanofluid-based cooling method for a hybrid photovoltaic/thermoelectric system is proposed in this work and it is compared with the conventional cooling methods experimentally. To this end, five different cooling methods were investigated experimentally, namely natural cooling, forced air cooling, water cooling, SiO_2/water nanofluid cooling, and Fe_3O_4/water nanofluid cooling. The results showed the promise of SiO_2/water nanofluid cooling, which yielded the highest power and efficiency, showing 54.29% and 3.35% improvement, while Fe_3O_4/water nanofluid cooling showed 52.40% and 3.13% improvement in power production and efficiency comparing with the natural cooling method, respectively.

Keywords: Hybrid PV/TE system; nanofluid cooling; total efficiency; thermoelectric.

1. Introduction

As a result of increasing energy demand and environmental concern, developing renewable energy technologies has received strong and sustained interest for a few decades. Solar energy is the most promising energy source for our future and solar photovoltaic (PV) technology, i.e. converting solar energy to electricity, has been widely used. However for PV cells, around two thirds of the solar energy is absorbed as heat, which is not only wasted but decreases the performance of the PV cells. It has been reported that the PV efficiency decreases around 0.5% for every degree of temperature increase of the panel (Tonui and Tripanagnostopoulos, 2008). Currently, Low conversion efficiencies and high costs of PV cells are the major obstacles for their large scale deployment (Hajji et al., 2017). Many studies have been performed with the aim of removing the heat produced by PV cells, or using electricity and thermal energy together, i.e. PVT technology((Li et al., 2016; Zhang and Xuan, 2016)). Thermoelectric devices, i.e. directly converting thermal energy into electricity under a temperature gradient, has shown great potential in cooling PV cells while providing extra electricity. Many experimental and numerical studies have been performed on photovoltaic–thermoelectric (PV/TE) hybrid systems in recent years (Bjørk and Nielsen, 2015; He et al., 2014; Rockendorf et al., 1999; Tayebi et al., 2014), some of which are briefly reviewed below.

Several novel hybrid systems are proposed and some of their aspects such as efficiency, performance, and manufacturing costs are investigated and compared in the literature. Wang et al. (Wang et al., 2011) proposed a novel PV/TE system composed of a solar selective absorption (SSA), dye-sensitized solar cells (DSSC), and a thermoelectric module (TEM) and experimentally studied the energy conversion efficiency of the system. Water was used as the coolant to create a temperature gradient between the hot and cold sides of TEM, and the result showed by using TEM, the overall efficiency of the system increased from 9.39% to 13.8%. Due to the low temperature gradient between the solar cell and the TEM, this model can be considered as a low grade heat source to produce electricity. Another type of PV/TE systems was investigated by Yang and Yin (Yang and Yin, 2011), where water flows inside a copper pipe that is located in the matrix of a phase-change material (PCM). They compared the efficiency of a single solar cell as well as a Photovoltaic/thermal (PVT) system with the PV/TE system at the same conditions, which showed a higher efficiency for the latter case. Since manufacturing costs besides efficiency also play and important role in the system's development justification,

Chavez-Urbiola (Chavez-Urbiola et al., 2012) experimentally investigated different configurations of solar cells and TEMs and compared their efficiencies as well as the manufacturing costs. In a novel attempt that used nanotubes for heat removal, a new model of PV/TE hybrid system was studied by Chang et.al (Chang et al., 2011), in which water was used as coolant for cooling the system and nanotubes made of copper oxide covered the cold side of the TEM. The results showed that using this design caused the temperature difference across the TEM to increase by 2K and the produced voltage to increase about 14.8%. Using a collector alongside the PV panel could improve the system performance. In this field, Deng et al. (Deng et al., 2013) proposed a new type of PV/TE system that utilized a bowl shaped collector and found that using this design greatly increased the energy conversion efficiency of the PV cell. Also, different types of PV panels and TEMs could be considered in such attempts. In this field Kossyvakis et al. (Kossyvakis et al., 2016) examined the performance of a tandem PV/TE system by employing poly-Si as well as dye-sensitized PV cells and indicated that the utilization of TEMs with shorter thermos-elements results in enhanced power output levels.

Apart from designing and investigating experimental setups from different aspects, some studies have theoretically investigated different PV/TE hybrid models and reported performance characteristics under various conditions. They also evaluated and compared the effects of different setup configurations on the overall performance of the system. Ju et al. (Ju et al., 2012) studied theoretically the effects of spectrum splitting of solar irradiance on the efficiency of PV/TE systems and showed that using this system is beneficial for high solar irradiance concentrations. The heat transfer mechanism could play an important role in the efficiency of such systems and in this field, Najafi and Woodburry (Woodbury, 2015) studied a theoretical model about heat transfer in a PV/TE system, where heat transfer mechanism was investigated at various layers of the hybrid system. A theoretical investigation on a PV/TE system was performed by Zhang et al. (Zhang and Chau, 2011a, 2011b) to investigate the effects of solar concentration on solar cell as well as the overall system efficiency. Finned structure was used to intensify the cooling of PV cells and the results showed that the overall efficiency can be increased by 1-8%. Dallan et al. (Dallan et al., 2015) showed that under the same radiation conditions, the efficiency of the PV/TE system increased to about 39% compared to a bare PV cell.

The electricity produced by TEM (depending on materials that are used in its structure) is too low comparing with a PV cell. However, TEM's role in the production of electricity will be increased by using the materials that have a higher figure of merit. Verma et al. (Verma et al., 2016) investigated the capability of a PV/TE system for power generation from waste heat of the PV panel in addition to the PV system's main generation As well as the effects of load disturbance and solar insolation variations on the performance of this system. In the case of theoretically assessing the effects of environmental conditions on the performance of such a system, Rezania et al. (Rezania et al., 2016) described a theoretical model of PV/TE system and showed that radiation losses from the outer surface of the PV cell as well as convective losses due to the wind blow on this surface caused critical effect on the efficiency of the PV/TE system.

In the field of nanofluids, the performed attempts are mostly theoretical. In one of such attempts, Wu et al. (Wu et al., 2015) established a theoretical model for estimating the performance of glazed/unglazed PV/TE system and served nanofluid as heat sink in order to enrich heat removal. The results showed that nanofluid improves the system efficiency comparing to water while the promotion is more significant for glazed systems. Khanjari et al. (Khanjari et al., 2017) evaluated the environmental parameters affecting the performance of photovoltaic thermal system using nanofluid and numerically investigated the using of nanofluid in a water-cooled PVT system (Khanjari et al., 2016). In the latter attempt, they showed that both thermodynamic first and second law efficiencies increase by increasing the nanoparticle volume fraction.

According to what we have cited in the literature review, most of the studies are focused in the cases of theoretical and numerical attempts to evaluate different methods of PV/TE system cooling. But, no specific and comprehensive study was found in the literature to experimentally investigate these methods, especially efficient nanofluids cooling methods, and their effects on PV/TE system performance characteristics. The present study is a novel experimental attempt, which aims to do so. In this study, five different cooling methods of the PV/TE system, namely natural air cooling, forced air cooling, pure water cooling, water-based SiO_2 nanofluid cooling, and water-based Fe_3O_4 nanofluid cooling are experimentally studied. The produced power and acquired efficiency are compared for each case and the corresponding efficiencies are compared.

2. Methodology

Error! Reference source not found. (a) and (b) shows schematic diagrams of the experimental setup, which shows air cooling and liquid cooling systems, respectively. In both systems, the PV cell absorbs solar irradiance and converts it into electricity. On the back side of the cell, a TEM is installed that uses the dissipated heat of the cell as the heat source, and liquid or air as the heat sink. Two air-based methods and three liquid-based methods are assessed in this work.

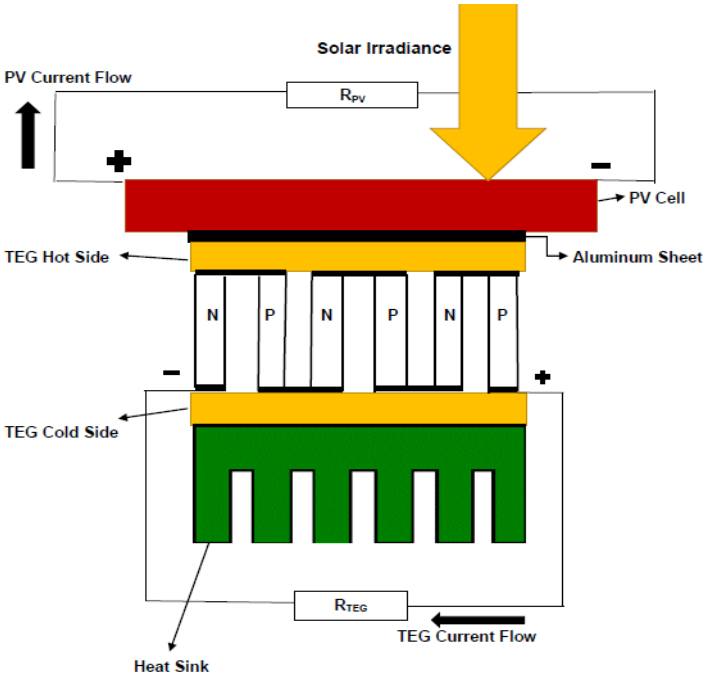

a) Hybrid PV-TE system with air cooling

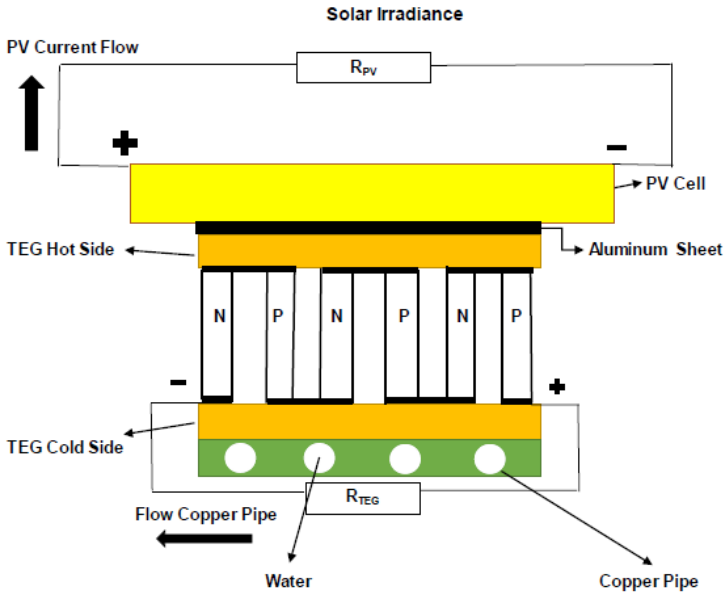

b) Hybrid PV-TE system with liquid cooling

Figure 1 Hybrid PV/TE system with a) air cooling, b) liquid cooling.

2.1. Materials

For this experiment, the crystalline silicon PV cell with dimensions of 30×15 cm^2 is utilized. It is manufactured by EVERSUN SOLAR TECHNOLOGY. The cell's characteristics are given in Table 1.

Table 1 PV cell characteristics

Parameter	Symbol	Value
Short circuit current	ISCR (A)	0.523
Open circuit voltage	V_{OC} (V)	22.56
Maximum power current	I_{MP} (A)	0.45
Maximum power voltage	V_{MP} (V)	11.5
Dimension	D (mm)	300×155×17
Weight	W (Kg)	0.65
Maximum power	P_{max} (W)	5
Efficiency	η (%)	15

For driving the flow of coolant liquid within the liquid cooling methods, a miniature pump was used, which consumed negligible power comparing with the produced power by the hybrid system. Also, one piece of TEM, TEC-1206, manufactured by Hebei I.T. (Shanghai) Co., Ltd is employed in the experiment. Bismuth Telluride was considered as the best thermoelectric material for the study considering its maximum operating temperature of about 90 ° C. The characteristics of the TEM are reported in Table 2. In order to collect the heat from the back side of the PV cell and efficiently transferring it to the hot side of TEM, an aluminum sheet was sandwiched between the PV cell and TEM.

In this section, the utilized equations for estimating the system efficiency are also presented. The efficiency of the PV cell is computed as follows (Skoplaki and Palyvos, 2009):

$$\eta_{cell} = \eta_{cell.ref}\left[1 - \beta_{ref}\left(T - T_{ref}\right)\right] \quad (1)$$

in which $\beta_{ref} = 0.0041°C^{-1}$, $\eta_{cell.ref} = 0.15$, and $T_{ref} = 25°C$ respectively represent the efficiency temperature coefficient, PV cell's efficiency, and the reference conditions' temperature. The TEM's efficiency is calculated as follows (Tse and Klug, 2006):

$$\eta_{max.TEM} = \frac{(T_H - T_C)}{T_H}\frac{(1 + ZT_M)^{0.5} - 1}{(1 + ZT_M)^{0.5} + \frac{T_H}{T_C}} \quad (2)$$

in which T_H, T_C, T_M, and Z represent hot side temperature, cold side temperature, average temperature, and figure of merit parameter, respectively. The latter is calculated as follows (Xi et al., 2007):

$$Z = \frac{S^2}{\rho K} \quad (3)$$

in which S, ρ, and K represent the Seebeck coefficient, TEM's electrical resistivity, and TEM's thermal conductivity, respectively. This constant figure of merit is used for the efficiency calculations and the required parameters are extracted from Table 12. Using the presented relation and constant values and the temperature gradient across TEM, which is presented later in section 3, the efficiency of TEM could be calculated.

Table 2 1206-TEC TEM parameters

Parameter	symbol	Value
Width	W (mm)	40±0.5/-0.2
Length	L (mm)	40±0.5/-0.2
Height	H (mm)	4±0.05
Wire length	WL (mm)	120
Flatness	F (mm)	0.02
Parallelism	P (mm)	0.03
Maximum voltage	V_{Max} (V)	4
Maximum current	I_{Max} (A)	24.4
Maximum power	Q_{Max} (W)	60
Maximum temperature gradient	DT_{Max} (°C)	70
Figure of merit	Z(1/K)	0.0085

2.2. Nanofluid preparation

Due to the possible presence of impurities, it is better to wash the nanoparticles with Hexane at first, and then put them in the oven with 80°C temperature for one day. For dispersing nanoparticle clots, the particles are milled for 30 minutes in a planetary-ball mill. The general procedure of preparing a nanofluid includes the following steps: at first, the nanoparticles are dispersed within the base fluid, which is water in our experiment, using a scoopula and a surfactant is added to the mixture if necessary, which prevents the nanoparticles from clotting within the base fluid bed. Finally, the mixture is placed in an ultrasonic cleaner, so the particles disperse within water uniformly.

Error! Reference source not found. and **Error! Reference source not found.** show the prepared nanofluids of SiO_2/water and Fe_3O_4/water, respectively. In order to prepare SiO_2/water nanofluid, Arabic gum is utilized as surfactant, while no surfactant is used for Fe_3O_4 preparation. Both nanofluids, which are homemade, are prepared with 0.5% mass ratio. For SiO_2/water nanofluid, the surfactant/nanoparticle ratio is 5%. The water base fluid volume was 700cc for both nanofluids. For SiO_2/water preparation the ultrasonic cleaner device with 80W power was used for 5 times, each time for 6 minutes, while for Fe_3O_4/water preparation, the device with

70W of power was used for 6 times, each time 6 minutes. Table 3 shows the nanofluids physical properties (Ferrouillat et al., 2011; Hosseinzadeh et al., 2015).

Table 3 Physical properties of SiO2 and Fe3O4 particles

Nanoparticles	Mean diameter (nm)	Density (kgm^{-3})	Thermal conductivity at 25 °C (Wm^{-1} K)	Specific heat at 25 °C (J/kg K)
SiO_2	22	2200	1.3	740
Fe_3O_4	50	5175	7	680

2.3. Setup assembly

In the hybrid system, an aluminum sheet was attached to the back side of the PV cell. TEM was then placed between the aluminum plate and a heat sink. For cooling the cold side of it, air cooled and liquid cooled systems are used. In the air-cooled system, natural air convection or a fan is used to cool the cold side of the TEM, while in the liquid cooled system, copper pipes are used as channels to flow liquid and dissipate heat from the cold side of the TEM, to which the pipes are connected by heat conductive glue. It should be noted that the current setup allows to take advantage of both cooling systems, either simultaneously or separately.

Six k-type thermocouple sensors are utilized in this setup for measuring different temperatures. The first sensor is placed on the outer surface of the PV cell exposed to solar irradiance, which measures the PV cell's surface temperature. The second sensor is placed at the back side of the PV cell. The third sensor is placed at the attachment location of the TEM's hot side and PV cell's back side. Considering negligible temperature difference measured among sensors 2 and 3, it is assumed that no heat loss takes place at the attachment location. The fourth sensor is attached to the cold side of TEM, which measures the TEM's cold side temperature during different cooling methods. The fifth and sixth sensors are placed at the beginning and the end of the copper pipe to measure the temperature of the coolant liquid both entering and exiting the hybrid system, which could be used to easily calculate the absorbed heat by the coolant liquid.

Also, two water-based nanofluid coolants, namely SiO_2/water and Fe_3O_4/water are utilized in addition to air and water coolant in order to evaluate the possible cooling and power extraction in the case of using nanofluids. To evaluate the effect of cooling system on the overall efficiency

and output power of the PV/TE system, all mentioned cooling systems are compared and the acquired results are presented and discussed.

The device type, measurement accuracy, and maximum standard uncertainty of the measurement apparatus are listed in Table 4. Assuming that the measurement error of the apparatus, as listed in Table 4, are negligible, the maximum uncertainties of the apparatus are calculated as follows:

$$u_{tools} = \frac{a}{\sqrt{3}} \tag{4}$$

Table 4 Measurement appratus specific data

Measurement apparatus	Device type	Measurement accuracy during tests	Maximum standard uncertainty
Multimeter-Voltage	UT71C/D/E	±(0.6%+1)V	0.046V
Multimeter-Current	UT71C/D/E	±(0.8%+1)A	0.051A
Radiometer	TES-1333	±(10W/m^2)+0.38W/m^2°C	2.99W/m^2
Thermocouple	K-types	±1°C	0.288°C
Liquid pump	AC/220-240V/8W	±1ml	0.288ml
Data record device	TESTO-177-T4,UK	±0.5°C	0.14°C

2.4. Data gathering process

At each stage of testing, the intensity of solar irradiance was measured and the data was recorded every half hour. Also, a thermocouple is used to measure the ambient temperature. The tests were performed over five days and each cooling method was tested in one full day, starting from august 23rd, during which no major weather fluctuations took place. It should be stated that in order to achieve similar weather conditions and consequent comparable data, the test was performed on several days and after investigating all the acquired data, it was revealed that these five days yielded the best comparable results. Figure 2 compares the solar irradiance during the five tested days. A TES-133 pyranometer is used for measuring the solar irradiance. Also, Figure 3 and Figure 4 show the wind speed as well as ambient temperature distribution during the same test days. The wind speed data are extracted from the Iran meteorological organization's database. It is found from the figures that the solar irradiance as well as the ambient temperature patterns of the test days are significantly similar to each other. Although, the wind speed pattern shows little differences during some hours of the day, the acquired results are still comparable, since the wind speed affects the natural cooling method more than others and the resultant

differences are negligible or justifiable. However, the wind speed is 1.5m/s at most measuring cases.

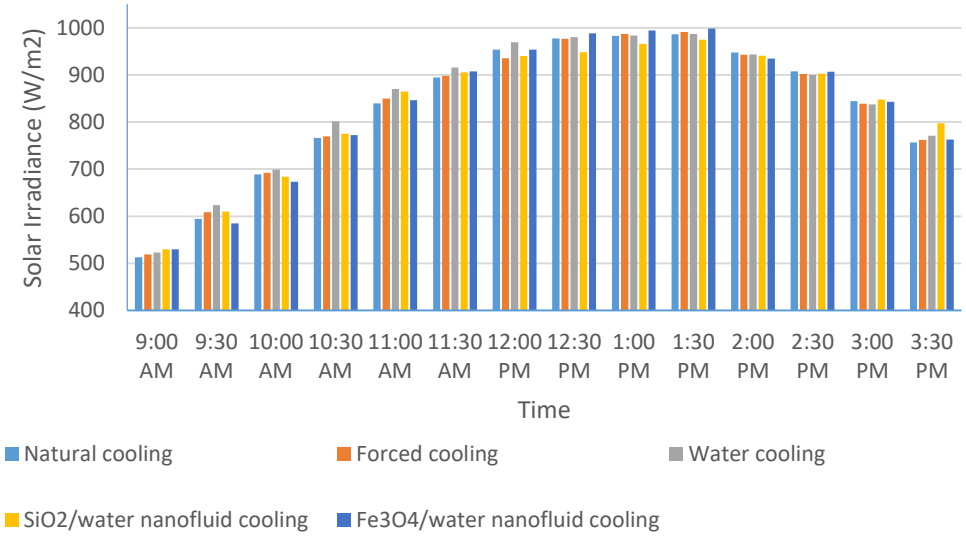

Figure 2 Solar irradiance distribution comparison during 5 test days

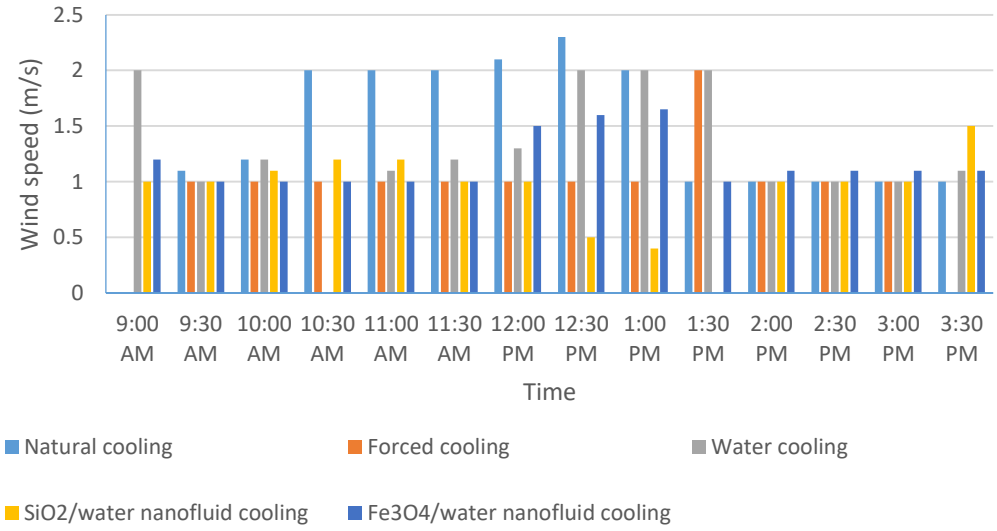

Figure 3 Wind speed distribution comparison during 5 test days

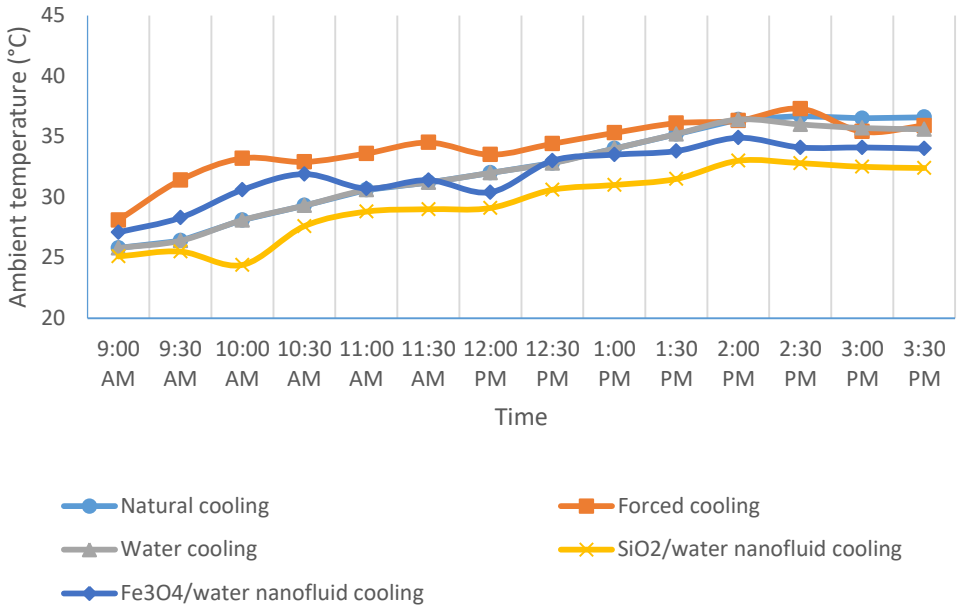

Figure 4 Ambient temperature distribution comparison during 5 test days

3. Results and discussions

The test is performed for 5 mentioned cases of natural, forced, water, SiO_2/water nanofluid, and Fe_3O_4/water nanofluid cooling, respectively. The PV cell's temperature as well as its produced power and efficiency are presented at the first section. After that the temperature gradient across TEM as well as its produced power and efficiency are presented. Finally, the produced power as well as the efficiency of the hybrid system are presented and compared for all cases and the improvement percentages of each cooling method are calculated and discussed using error analysis methods.

3.1. PV cell's results

In this section, the voltage, surface temperature variation, produced power, and the efficiency of the PV cell are discussed for five cooling cases. Figure 5 shows the PV cell's surface temperature during 5 testing days. It is observed from the figure that at most cases, the temperatures are lower for nanofluid cooling methods, which shows more efficient cooling. However, the effect of the cooling method on the cell's surface temperature is mostly about 10°C. Also, Figure 6 shows the produced voltage by the PV cell for the natural cooling case as a sample. It is clear that the cell's produced voltage has direct relation with the solar irradiance radiated on the panel, which

increases until noon and decreases gradually in the afternoon. It should be noted that the PV cell's voltage as well as its efficiency increase with irradiance increase, but decrease with temperature increase. The PV cell's voltage reaches to a maximum value of about 16.8V. Negligible variation is observed for the produced current by the cell which is about 0.325A.

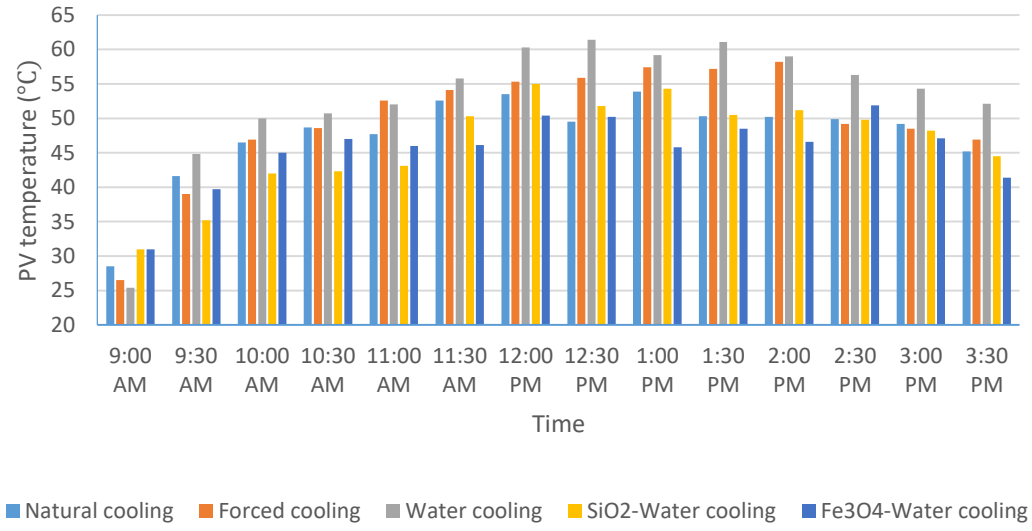

Figure 5 PV cell's surface temperature for 5 cooling methods

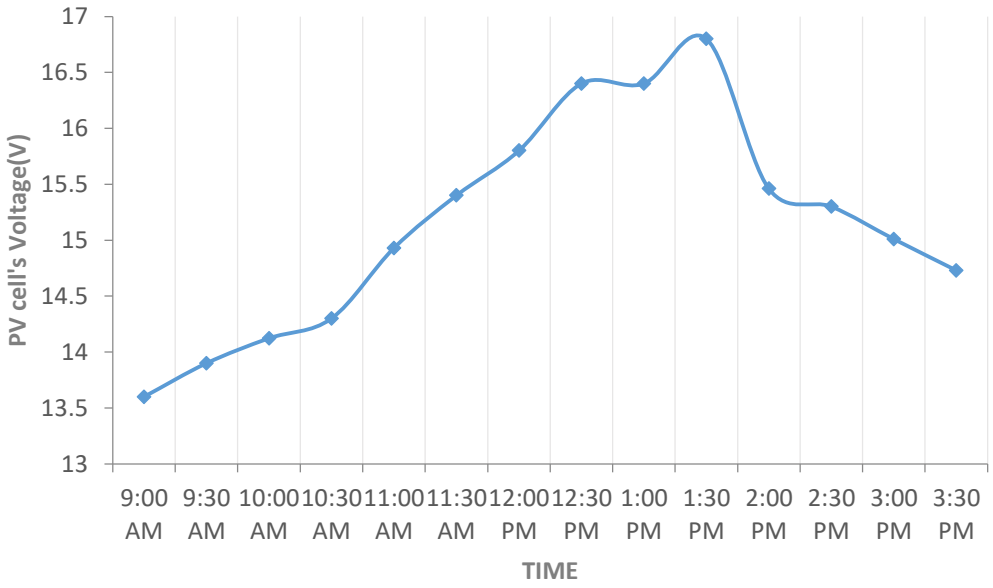

Figure 6 Solar PV cell voltage during the test day

Figure 7 shows the produced power of the cell. It is observed from the figure that the produced power by the PV cell does not vary significantly with the cooling method. It was expected since

the cooling method mostly affects the temperature of the cold side of the TEM. In all methods, as the solar irradiance increase the produced power by the PV cell increases and then slightly decreases, which is due to temperature increase of the cell and it then increases again and finally decreases at the final hours of the test as the solar irradiance decreases during the afternoon. Still, lower produced power is observed for the natural cooling method comparing with others, which is due to lower cooling take place for the cell, reducing its efficiency and its produced power. Again it should be noted that temperature increases has a negative effect on the cell's produced voltage despite the solar irradiance having a positive effect and the produced voltage is determined by the interaction of these two opposite parameters. Therefore, it could be noted that the cooling method indirectly affects the PV cell's performance by lowering its temperature.

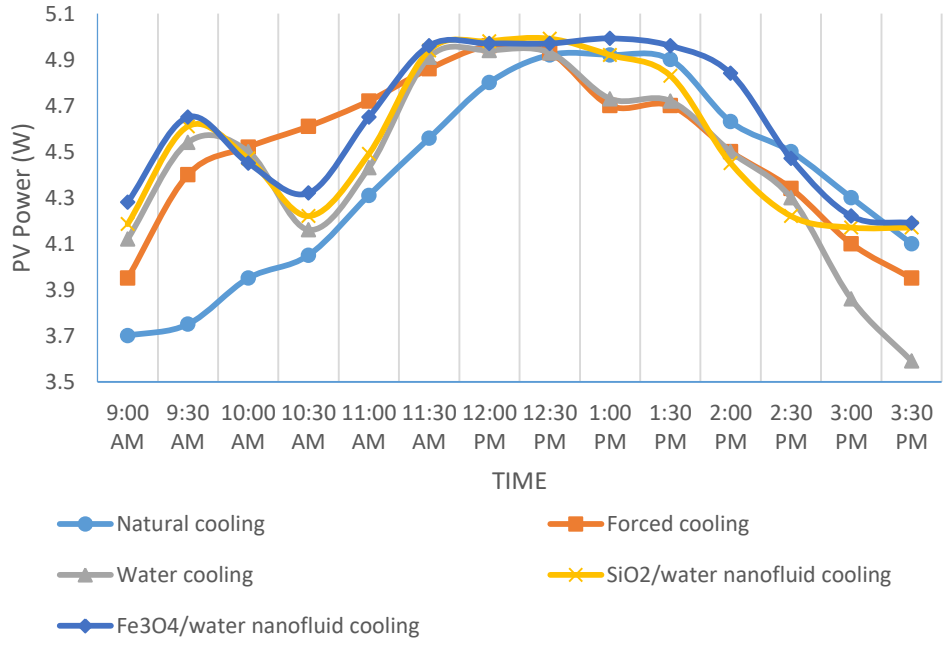

Figure 7 Produced power by PV cell for all cooling methods during times of the day

Figure 8 shows the PV cell's efficiency for 5 cooling methods in one chart. It is observed from Figure 8 that the cell's efficiency gradually decreases during the day due to temperature increase. Although, the decrease rate is not similar for all cooling methods, but variations of the efficiency among methods is not significant, proving that the cell's performance is not heavily affected by the utilized cooling method. In other words, the TEM's cooling method indirectly affects the cell's efficiency and it is observed that SiO_2/water nanofluid cooling method provides the highest

efficiency. This is because more efficient cooling decreases the cell's performance temperature leading to higher efficiencies. Also, the maximum efficiency of the cell is for the lowest surface temperature, which is about 14.9%.

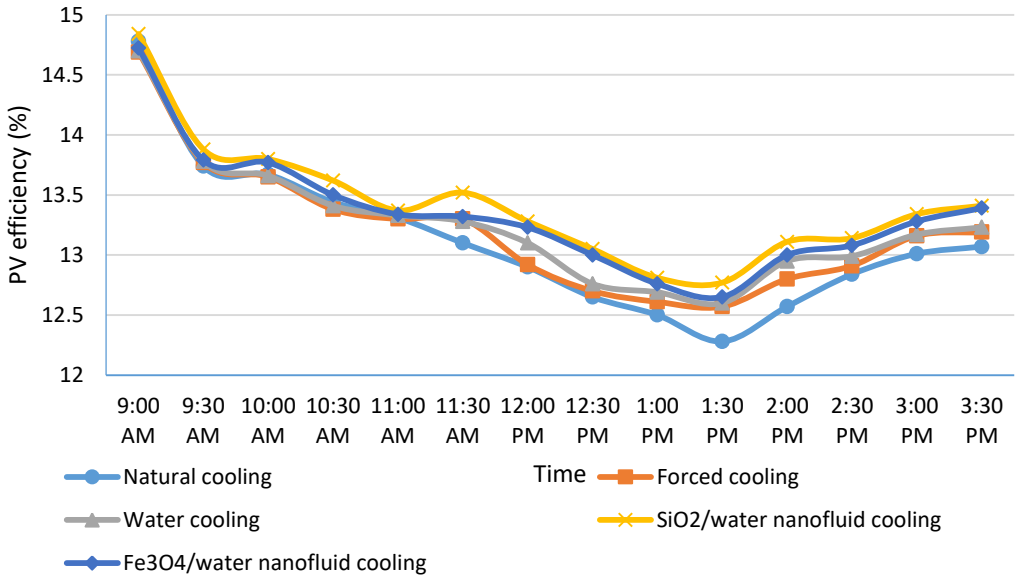

Figure 8 PV cell's efficiency for different cooling methods during times of the day

3.2. TEM's results

In this section, temperature gradient, produced voltage, produced power, and the efficiency of the TEM are presented and discussed for five cooling cases. Figure 9 shows the produced voltage of the TEM for natural cooling as a sample. TEM's voltage depends on the temperature gradient across hot and cold ends, which in turn depends on PV cell's backside temperature and the cooling method. It is observed from the figure that at the beginning of the experiment at 9:00AM, TEM's voltage is low, about 1.1V, due to lower solar irradiance and consequent lower temperature gradient across the module; however, as the solar irradiance increases during the day, the backside temperature of the cell, which is the TEM's hot side temperature, increases and consequently, the temperature gradient across TEM increases leading to higher voltages, reaching a maximum of about 1.64V, while the produced current is approximately constant at about 3.01A. In the afternoon, as the solar irradiance decreases, it is obvious that TEM's voltage also decreases. For gaining a better insight into the effects of the temperature gradient across the

TEM on the produced voltage, power, and efficiency, this gradient is compared for all cooling methods in Figure 10. As observed from the figure, as the solar irradiance increases, the TEM's hot side temperature increases and if no major fluctuations in wind speed take place, the temperature gradient gradually increases. The more efficient the utilized cooling method, higher temperature gradients are obtained. It is seen from the figure that SiO_2/water nanofluid cooling is the most efficient method providing highest temperature gradients. After that Fe_3O_4/water nanofluid, water, forced, and natural cooling are placed, respectively. Also, it is seen that using a fan for forced cooling provides better heat removal than natural cooling as expected.

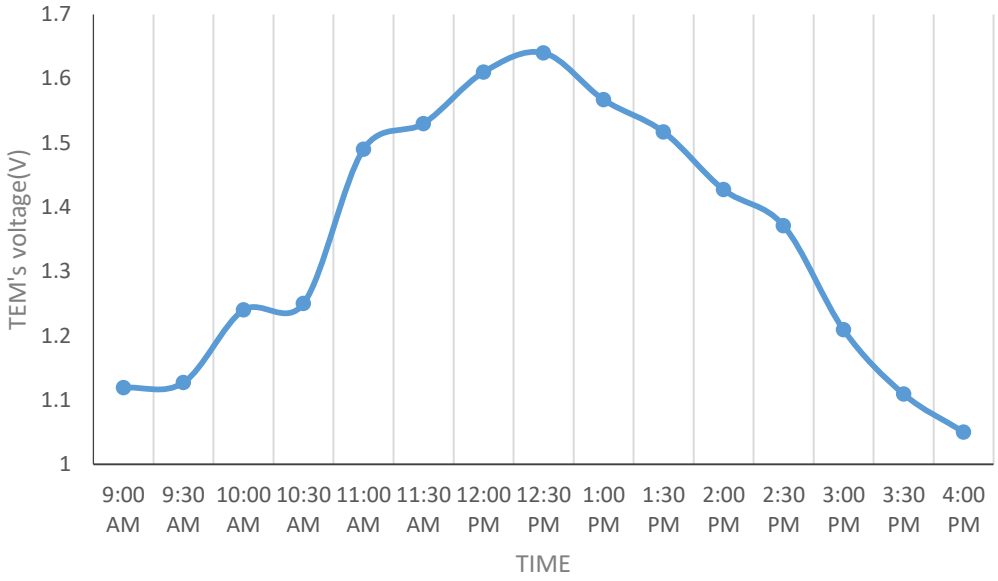

Figure 9 TEM's voltage during the test day for natural cooling

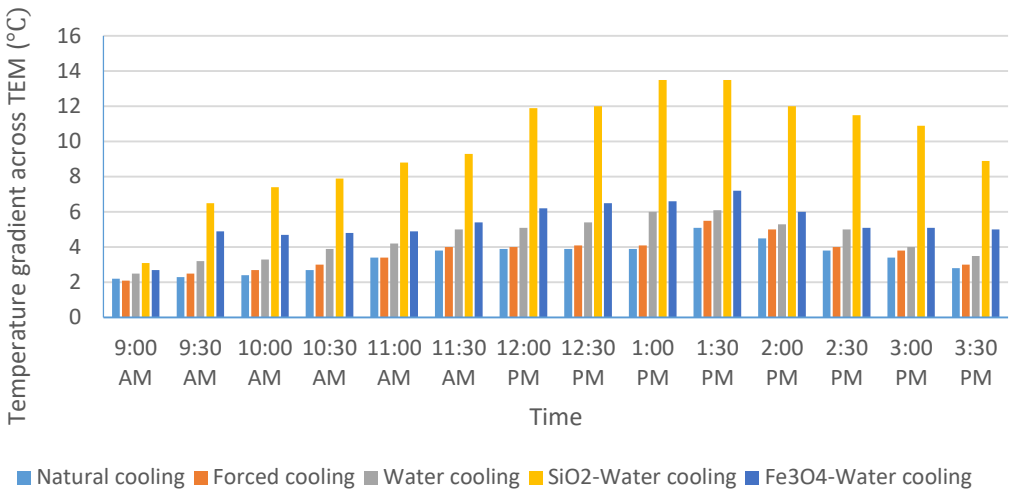

Figure 10 Temperarure gradient across TEM during the day for 5 cooling cases

Figure 11 compares the produced voltage of the TEM for all cooling cases at 12:30 p.m. As mentioned before, TEM's voltage depends on the temperature gradient across hot and cold ends. Therefore, higher voltages means higher temperature gradients. As is observed from the figure, the SiO_2/water nanofluid cooling method produces the highest voltage, which means the most powerful cooling among all method. Also, it is seen that using Fe_3O_4 nanoparticles in water enhances cooling comparing with pure water and at next places forced cooling and natural cooling are placed, respectively.

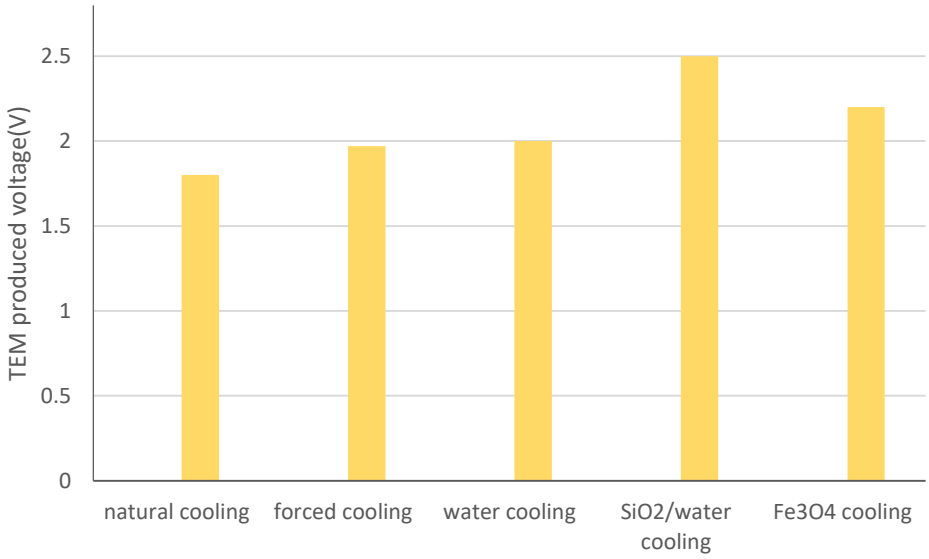

Figure 11 TEM's produced voltage at 12:30PM for all cooling methods

Figure 12 shows the produced power by the TEM for all cooling methods. As the solar irradiance increase over time, the temperature gradient across the TEM increases, and consequently the produced power increases reaching a maximum value of 5.57W. It is seen that after around 12:30 p.m. the TEM's power gradually decreases. It is seen that the power curve is in complete accordance with the temperature gradient curve, which shows a direct relation. The instant power reduction of TEM in the afternoon for natural cooling method is a result of irradiance reduction as well as wind speed reduction, which facilitates the natural cooling process.

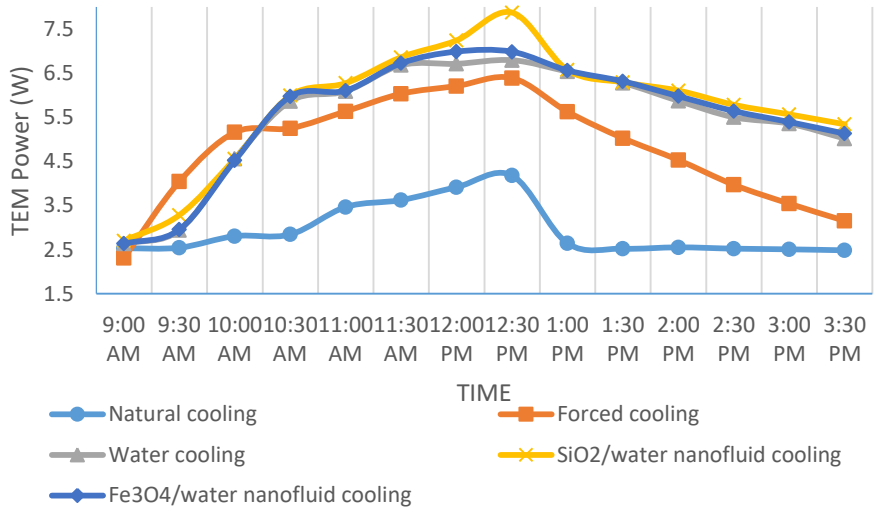

Figure 12 TEM's produced power for all cooling methods during different times of a day

Figure 13 shows the TEM's efficiency during the daily hours for all 5 cooling methods. It is seen from the figure that SiO_2/water nanofluid cooling yields maximum efficiency and Fe_3O_4/water nanofluid cooling takes the next place. As observed in section 2, the efficiency of TEM depends on the temperature gradient across the device and higher temperature gradients across the device lead to higher efficiencies. Also, it is seen that forced and natural cooling methods have negligible difference in the field of TEM efficiency.

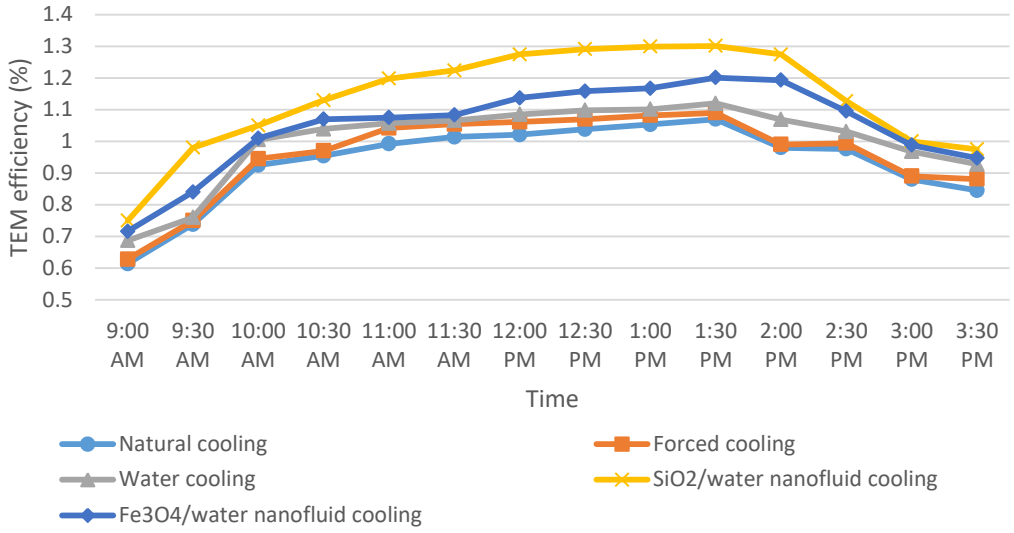

Figure 13 TEM's efficiency for different cooling methods during times of the day

3.3. Power and efficiency of the hybrid system

In this section, the produced power and efficiency of the hybrid system are compared and discussed for all cooling methods. **Error! Reference source not found.** shows the produced power by the hybrid system. It is seen from the figure that using a fan for removing heat causes significant power increase comparing with natural cooling method. Also, using water circulation for cooling causes significant power increase comparing with air cooling. However, the difference between liquid cooling methods in power production is negligible. The maximum produced power is for SiO_2/water nanofluid cooling method, which takes place at 12:30 p.m. The sudden decrease of the power production at 12:30 p.m. in natural cooling method is caused by wind speed reduction at that time, which is obvious in Figure 3 for natural cooling between 12:30 p.m. and 1:30 p.m.

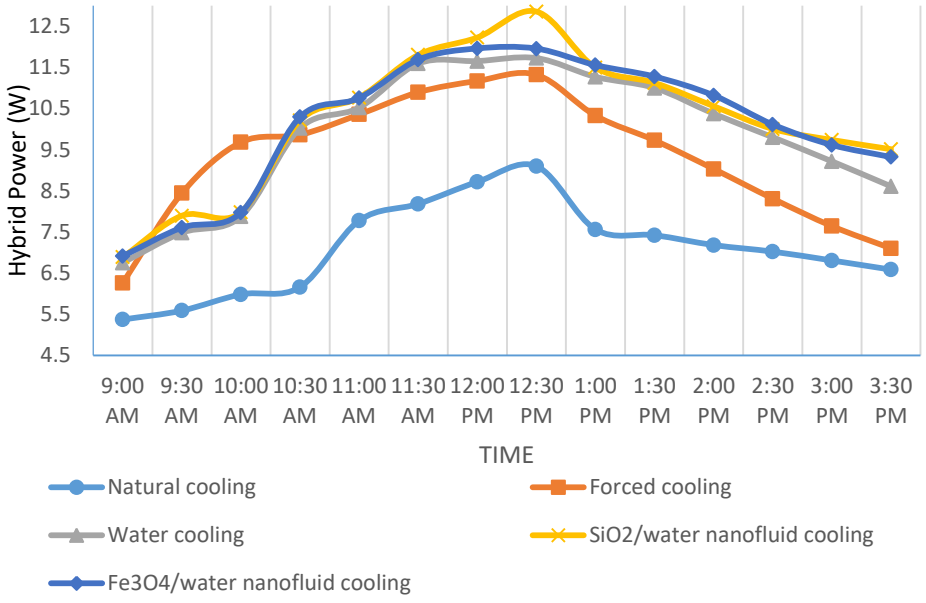

Figure 14 Hybrid system producd power for all cooling methods during different hours of a day

Figure 15 shows the efficiency of the hybrid system for all cooling methods. It is observed from the figure that natural cooling has the lowest and SiO_2/water cooling has the highest efficiencies. However, the total difference is lower than 2% during all hours of the test. It should be noted that higher efficiency does not necessarily mean higher power production value, since as the solar irradiance increases the amount of power production increases, but the efficiency of the system gradually decreases due to temperature increases of the PV panel mainly and it is clear that the major part of the hybrid system efficiency is dedicated to the PV panel, since the TEM has low

value efficiencies (of the order of 1%). This is because the temperature gradient across the TEM does not exceed 14°C, which is a low temperature gradient to produce power with a TEM.

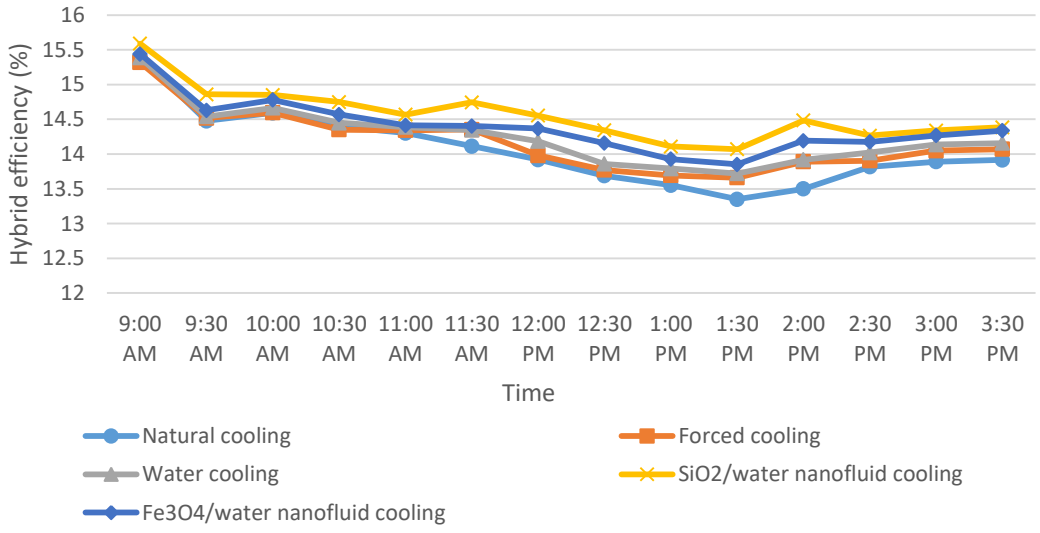

Figure 15 Hybrid system efficiency for all cooling methods during daily hours

For better reporting the acquired improvement in power production via using different cooling methods, the improvement percentage is calculated and reported. To this end, natural cooling is considered as the base cooling method and mean relative error (MRE) statistical error analysis formula is used to calculate the improvement percentage (Kasaeian et al., 2016), as follows:

$$MRE = \frac{1}{y}\sum_{i=1}^{y}\left|\frac{e_i - m_i}{m_i}\right| \quad (4)$$

in which y, e, and m represent number of acquired data during the test day, deviation from the base state value, and the value for the base state, respectively. Table 5 and Table 6 show the yielded improvement via using different cooling methods relative to the natural cooling method, which is considered as the base state. It is seen in Table 5 that the maximum power increase corresponds to SiO_2/water nanofluid cooling method, which shows 54.29% improvement relative to the natural cooling case. Also, the same methods shows the maximum efficiency improvement, which is 3.55% relative to the natural cooling case. It is again obvious that improvement percentage in power production is an order higher comparing with the developed efficiency improvement. The next place goes for Fe_3O_4/water nanofluid cooling method with

52.397% power production improvement and 3.131% efficiency improvement relative to the natural cooling method as the base state.

Table 5 Power production improvment for all methods relative to the natural cooling case

Total power	Natural cooling	Forced cooling	Water cooling	SiO_2/water nanofluid cooling	Fe_3O_4/water nanofluid cooling
MRE (%)	base	4.885	5.776	8.26	6.284

Table 6 Efficiency improvement for all methods relative to the natural cooling case

Total efficiency	Natural cooling	Forced cooling	Water cooling	SiO_2/water nanofluid cooling	Fe_3O_4/water nanofluid cooling
MRE (%)	Base	1.865	3.051	3.355	3.131

It is observed from the acquired results that the cooling performance of SiO_2/water nanofluid is generally better than Fe_3O_4/water nanofluid. The reason to this issue could be traced in two fields. First, according to the performed experimental and mathematical investigations, the convective heat transfer coefficient of the SiO_2/water nanofluid is higher than that of Fe_3O_4/water nanofluid (Hosseinzadeh et al., 2015). The second and more important reason is that Fe_3O_4/water nanofluid shows best heat transfer coefficient when placed under a magnetic field, which is investigated in several related attempts (Amani et al., 2017) and in the absence of a magnetic field, SiO_2/water nanofluid shows better heat convection performance.

4. Conclusions

In this study, the produced power and efficiency of a hybrid system, consisting of a photovoltaic cell and a thermoelectric module, were investigated experimentally for five different cooling methods for the TEM's cold side, namely natural cooling, forced cooling, water cooling, SiO_2/water nanofluid cooling and Fe_3O_4/water nanofluid cooling. The experiments were performed in five days when the weather difference such as the solar irradiance, wind speed, and ambient temperature variations were negligible. The results are presented for PV cell, TEM, and the hybrid system separately. Based on the acquired experimental results, the following conclusions could be drawn:

- Liquid cooling methods yielded significantly better results for the total power of the hybrid system comparing with the air cooling methods. Water cooling method produced 47.7% more power comparing with the natural cooling method.
- For water based methods, using nanofluid increased the cooling performance and consequently the total produced power. For example, SiO_2 and Fe_3O_4 nanofluids had an average improvement of 5.7% in power production comparing with pure water cooling method.
- SiO_2 nanofluid achieved slightly high power production relative to Fe_3O_4/water nanofluid, i.e., 0.971%. This could be due to a higher convective heat transfer coefficient from SiO_2 nanofluid.
- The cooling method mainly affected the TEM performance, and indirectly affected the PV cell's performance by lowering its temperature and consequently increasing the produced power and efficiency. Therefore, better cooling methods such as SiO_2/water and then Fe_3O_4/water nanofluid cooling methods provided slightly better performance for the PV cell.

Integration of PV cell with TEM cooled by nanofluids could be used in the future for distributed power production purposes. As an interesting topic for research in this field, the nanofluid cooling methods could be investigated by exposing to a magnetic field. Under such a circumstances, the nanofluid convective heat transfer coefficients could be intensified, leading to improved power production performance.

References

Amani, M., Ameri, M., Kasaeian, A., 2017. Investigating the convection heat transfer of Fe_3O_4 nanofluid in a porous metal foam tube under constant magnetic field, Experimental Thermal and Fluid Science. doi:10.1016/j.expthermflusci.2016.12.003

Bjørk, R., Nielsen, K.K., 2015. The performance of a combined solar photovoltaic (PV) and thermoelectric generator (TEG) system. Sol. Energy 120, 187–194. doi:10.1016/j.solener.2015.07.035

Chavez-Urbiola, E.A., Vorobiev, Y. V., Bulat, L.P., 2012. Solar hybrid systems with thermoelectric generators. Sol. Energy 86, 369–378. doi:10.1016/j.solener.2011.10.020

Chang, H., Kao, M.J., Cho, K.C., Chen, S.L., Chu, K.H., Chen, C.C., 2011. Integration of CuO thin films and dye-sensitized solar cells for thermoelectric generators. Curr. Appl. Phys. 11,

S19–S22. doi:10.1016/j.cap.2010.12.039

Dallan, B.S., Schumann, J., Lesage, F.J., 2015. Performance evaluation of a photoelectric-thermoelectric cogeneration hybrid system. Sol. Energy 118, 276–285. doi:10.1016/j.solener.2015.05.034

Deng, Y., Zhu, W., Wang, Y., Shi, Y., 2013. Enhanced performance of solar-driven photovoltaic-thermoelectric hybrid system in an integrated design. Sol. Energy 88, 182–191. doi:10.1016/j.solener.2012.12.002

Ferrouillat, S., Bontemps, A., Ribeiro, J.P., Gruss, J.A., Soriano, O., 2011. Hydraulic and heat transfer study of SiO2/water nanofluids in horizontal tubes with imposed wall temperature boundary conditions. Int. J. Heat Fluid Flow 32, 424–439. doi:10.1016/j.ijheatfluidflow.2011.01.003

Hajji, M., Labrim, H., Benaissa, M., Laazizi, A., Ez-Zahraouy, H., Ntsoenzok, E., Meot, J., Benyoussef, A., 2017. Photovoltaic and thermoelectric indirect coupling for maximum solar energy exploitation. Energy Convers. Manag. 136, 184–191. doi:10.1016/j.enconman.2016.12.088

He, W., Zhou, J., Chen, C., Ji, J., 2014. Experimental study and performance analysis of a thermoelectric cooling and heating system driven by a photovoltaic/thermal system in summer and winter operation modes. Energy Convers. Manag. 84, 41–49. doi:10.1016/j.enconman.2014.04.019

Hosseinzadeh, M., Heris, S.Z., Beheshti, A., Shanbedi, M., 2015. Convective heat transfer and friction factor of aqueous Fe3O4 nanofluid flow under laminar regime. J. Therm. Anal. Calorim. 124, 1–12. doi:10.1007/s10973-015-5113-z

Ju, X., Wang, Z., Flamant, G., Li, P., Zhao, W., 2012. Numerical analysis and optimization of a spectrum splitting concentration photovoltaic-thermoelectric hybrid system. Sol. Energy 86, 1941–1954. doi:10.1016/j.solener.2012.02.024

Kasaeian, A., Barghamadi, H., Pourfayyaz, F., 2016. Performance comparison between the geometry models of multi-channel absorbers in solar volumetric receivers. Renew. Energy 105, 1–12. doi:10.1016/j.renene.2016.12.038

Khanjari, Y., Kasaeian, A.B., Pourfayaz, F., 2017. Evaluating the environmental parameters affecting the performance of photovoltaic thermal system using nanofluid. Appl. Therm. Eng. 115, 178–187. doi:10.1016/j.applthermaleng.2016.12.104

Khanjari, Y., Pourfayaz, F., Kasaeian, A.B., 2016. Numerical investigation on using of nanofluid in a water-cooled photovoltaic thermal system. Energy Convers. Manag. 122, 263–278. doi:10.1016/j.enconman.2016.05.083

Kossyvakis, D.N., Voutsinas, G.D., Hristoforou, E. V., 2016. Experimental analysis and performance evaluation of a tandem photovoltaic-thermoelectric hybrid system. Energy Convers. Manag. 117, 490–500. doi:10.1016/j.enconman.2016.03.023

Li, G., Zhao, X., Ji, J., 2016. Conceptual development of a novel photovoltaic-thermoelectric system and preliminary economic analysis. Energy Convers. Manag. 126, 935–943. doi:10.1016/j.enconman.2016.08.074

Rezania, A., Sera, D., Rosendahl, L.A., 2016. Coupled thermal model of photovoltaic-thermoelectric hybrid panel for sample cities in Europe. Renew. Energy 99, 127–135. doi:10.1016/j.renene.2016.06.045

Rockendorf, G., Sillmann, R., Podlowski, L., Litzenburger, B., 1999. PV-hybrid and thermoelectric collectors. Sol. Energy 67, 227–237. doi:10.1016/S0038-092X(00)00075-X

Skoplaki, E., Palyvos, J.A., 2009. On the temperature dependence of photovoltaic module electrical performance: A review of efficiency/power correlations. Sol. Energy 83, 614–624. doi:10.1016/j.solener.2008.10.008

Tayebi, L., Zamanipour, Z., Vashaee, D., 2014. Design optimization of micro-fabricated thermoelectric devices for solar power generation. Renew. Energy 69, 166–173. doi:10.1016/j.renene.2014.02.055

Tonui, J.K., Tripanagnostopoulos, Y., 2008. Performance improvement of PV/T solar collectors with natural air flow operation. Sol. Energy 82, 1–12. doi:10.1016/j.solener.2007.06.004

Tse, J.S., Klug, D.D., 2006. Recent Trends for the Design and Optimization of Thermoelectric Materials - A Theoretical Perspective, Thermoelectrics Handbook: Macro to Nano. doi:10.1201/9781420038903.ch31

Verma, V., Kane, A., Singh, B., 2016. Complementary performance enhancement of PV energy system through thermoelectric generation. Renew. Sustain. Energy Rev. 58, 1017–1026. doi:10.1016/j.rser.2015.12.212

Wang, N., Han, L., He, H., Park, N.-H., Koumoto, K., 2011. A novel high-performance photovoltaic–thermoelectric hybrid device. Energy Environ. Sci. 4, 3676. doi:10.1039/c1ee01646f

Woodbury, K., 2015. Modeling and Analysis of a Combined Photovoltaic-Thermoelectric Power Generation System 1–7.

Wu, Y.Y., Wu, S.Y., Xiao, L., 2015. Performance analysis of photovoltaic-thermoelectric hybrid system with and without glass cover. Energy Convers. Manag. 93, 151–159. doi:10.1016/j.enconman.2015.01.013

Xi, H., Luo, L., Fraisse, G., 2007. Development and applications of solar-based thermoelectric technologies. Renew. Sustain. Energy Rev. 11, 923–936. doi:10.1016/j.rser.2005.06.008

Yang, D., Yin, H., 2011. Energy conversion efficiency of a novel hybrid solar system for photovoltaic, thermoelectric, and heat utilization. IEEE Trans. Energy Convers. 26, 662–670. doi:10.1109/TEC.2011.2112363

Zhang, J., Xuan, Y., 2016. Investigation on the effect of thermal resistances on a highly concentrated photovoltaic-thermoelectric hybrid system. Energy Convers. Manag. 129, 1–10. doi:10.1016/j.enconman.2016.10.006

Zhang, X., Chau, K.T., 2011a. An automotive thermoelectric-photovoltaic hybrid energy system using maximum power point tracking. Energy Convers. Manag. 52, 641–647. doi:10.1016/j.enconman.2010.07.041

Zhang, X., Chau, K.T., 2011b. Design and Implementation of a New Thermoelectric-

Photovoltaic Hybrid Energy System for Hybrid Electric Vehicles Design and Implementation of a New Thermoelectric-Photovoltaic Hybrid Energy System for Hybrid Electric. Electr. Power Components Syst. 36, 511–525. doi:10.1080/15325008.2010.528530